Supplementary Material (ESI) for New Journal of Chemistry

Supplementary Information Available for

Lewis Acid Effects on Donor/Acceptor Associations and Redox Reactions: Ternary Complexes of Heteroaromatic N-Oxides with Boron Trifluoride and Organic Donors

Yakov Nizhnik, Jian Jiang Lu, Sergiy V. Rosokha, and Jay K. Kochi

Department of Chemistry, University of Houston, Houston, TX, 77204

IR spectral data for NQO and NPO N-oxides and their associates (Table S1 and S2), spectral characteristics of NPO and NQO and their complexes with BF_3 in acetonitrile (Table S3), oxidation potentials of various organic donors and wavelength of charge-transfer bands of their complexes with NPO·BF_3 adducts (Table S4), reduction potentials of various organic acceptors and wavelength of charge-transfer bands of their complexes with pyrene and anthracene (Table S4) donor/acceptor stacking (Fig. S1), spectral deconvolution for NPO/anthracene solutions (Fig. S2), spectra of pyrene/NPO solutions (Fig. S3), spectra of NXO/BF_3 solutions (Fig. S4), cyclic voltammogramms of NPO, NQO and their mixtures with BF_3 (Fig. S5), results of spectral titrations in the phenothiazine : NXO : BF_3 systems (Fig. S6), illustration of oxygen hybridization (Fig. S7) and resonance contributors (Fig. S8) of N-oxide molecules, N-O-B angles in the reported N-oxide complexes (Table S6).

Table S1. IR-spectral data for NPO N-oxide, pyrene, and their associates

pyrene	NPO	$(Pyrene)_2 \cdot NPO$	$NPO \cdot BF_3$	$pyrene \cdot NPO \cdot BF_3 \cdot CH_2Cl_2$
	3114 w	3108 w	3136, 3125 w	3133 w
	3078 w	3088 w	3086 w	
3047 w	3045 w	3048 w	3075 w	3047 w
	3027 w	3027 w	3051 w	
	1602 m	1598 w	1618 w	1598 m
	1585 w	1583 w	1612 w	1596 w
		1522 w	1545 s	1546 s
	1508 s	1509 s	1484 m	1485 w
	1460 m	1464 m	1449 w	1434 w
1433 w		1435 w	1355 m	1357 m
	1364 w	1345 m	1251 s	1265 w
	1345 vs	1334 m	1214 w	1241 m
	1284 m	1291 m	1180 m	1185 w
	1269 vs	1284 vs	1113 s	
	1232 w	1244 w	1149 s	1165 m
1184 w		1185 w	1127 w	
	1174m	1171 m	1109 w	
	1170 m			
	1122 s	1113 s	1080 s	
	1096 m	1097 w	1043 w	1073 w
	1018 w	1024 w	1008 w	
963 w	960 w	962 w	977 m	962 m
	876 w		953 m	958 m
	862 s	868 w	937 m	929 m
837 vs		845 vs	911 s	911 m
819 w	829 w	821 w	882 m	875 m
748 m	749 m	760, 753 m	871 s	865 s
708 vs		713 vs	836 w	849 m
	680 m	679 w		837 vs
			748 w	749 m
			739m	735m
			735,5 m	731 m
				707 vs
			681 m	676 m

Table S2. IR-spectral data for NQO, NQO·BF_3 and pyrene ·NQO·BF_3·CH_2Cl_2

pyrene	NQO	NQO·BF_3	NQO·BF_3·(pyrene)2
	3126 w	3131 w	3128 w
	3099 w	3110 w	3100 w
3047 w	1588 w	1620 w	
	1565 m	1604 w	1598 w
	1518 s	1540 s	1540 m
	1507.5 m	1521 w	1520 w
	1498 w,		
	1445 w		
	1427 m-w	1435 w	1433 w
	1388 m	1393 w	1396 w
1433 w	1356 w	1364 sh	1369 sh
	1342 m	1356 m	1360
	1333 m	1339 m	1339 w
	1297 sh. vs,	1274 w	1270 w
	1293 vs		
	1258 w		
	1237 m	1223 w	1243 w
		1203 w	
1184 w	1200 w	1207	1207 w
	1163 w	1165 sh	
	1156 m,1129 w	1152 m, 1136 m	1140 m
	1068 w	1113 w	1103 m
		1074 s	1074 m
		1054 m	1058 w
	1030 w	1036 w	1033 w
	1000 w	990 sh	
	988 w	981 w	985 w
963 w	967 w, 938 w	965 m, 940 w	961 w
	926 w	915 s broad	918 w
	876 w	873, 856 w	885 s broad
837 vs	836 sh, 829 s	834 s	845 vs
819 w	787 w	781 w	768 w
	769 w	775 vs	768 m
748 m	764 vs	763 s	757 s
708 vs	736 s,	723 w	724 w,
	722 w		711 vs

Table S3. Spectral characteristics of NPO and NQO N-oxides and its complexes with BF_3 in acetonitrile.

	λ_{max}, nm (log ε)
NPO	237 (3.97), 344 (4.22)
NPO·BF_3	240 (4.02), 280 sh (3.59)
NQO	259 (4.22), 386 (4.11)
NQO·BF_3	242 (4.35), 330 (3.78)

Table S4. Oxidation potentials of various organic donors and wavelength of charge-transfer bands of their complexes with NPO·BF_3 adducts

Donor	$E_{ox}^{1/2}$, V[a)]	λ_{max}, nm
Octamethylbiphenylene	+0.82	680
9,10-Dimethylanthracene	+0.94	580
9,10-Dimethoxyanthracene	+0.98	550
Anthracene	+1.09	511
Pyrene	+1.16	500
1,4-dimethoxybenzene	+1.35	455
Naphthalene	+1.54	420
Hexaethylbenzene	+1.59	406
Hexamethylbenzene	+1.62	439
Penrtamethylbenzene	+1.71	410

a) From ref. 27

Table S5. Reduction potentials of various acceptor[a] and wavelength of charge-transfer bands of their complexes with anthracene and pyrene donors.

Acceptor	E_{red}, V vs SCE	λ_{max}, nm [Anthracene, A]	[Pyrene, A]
2,3-dichloro-5,6-dicyano-*p*-benzoquinone[a]	0.52	885	840
tetracyanoethylene[a]	0.17	718	720
tetracyanopyrazine	-0.24	580	583
p-bromanil	-0.063	634	615
tetracyanoquinodimethane[a]	0.19	763	739
p-chloranil[a]	-0.02	635	612
o-chloranil	0.15	679	653
o-bromanil	0.083	690	664
2,3-dicyano-*p*-benzoquinone	0.257	747	724
tetrafluorotetracyanoquinodimethane	0.543	990	942
trinitrobenzene	-0.6[b]	446	439
2,6-dichloro-*p*-benzoquinone	-0.194	555	536
p-fluoranil	-0.07	593	571
tropilium	-0.18[b]	538	537
2,3-dibromo-5,6-dicyano-*p*-benzoquinone	0.5	879	846

a) From ref. 27; b) From R. Rathore, S.V. Lindeman and J.K.Kochi, *J. Am. Chem. Soc.* **1997,** *119,* 9393.

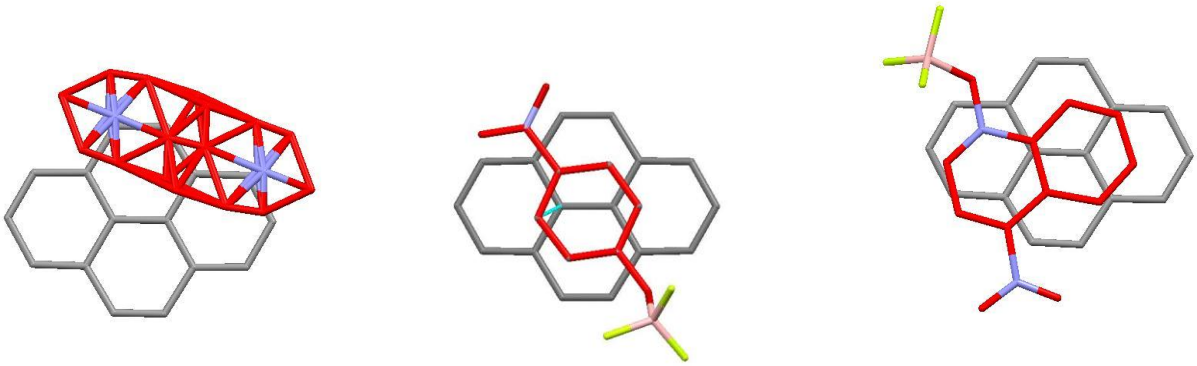

Fig. S1. Donor/acceptor stacking in A) $(pyrene)_2 \cdot NPO$; B) $pyrene \cdot NPO \cdot BF_3$ and C) $(pyrene)_2 \cdot NQO \cdot BF_3$ salts.

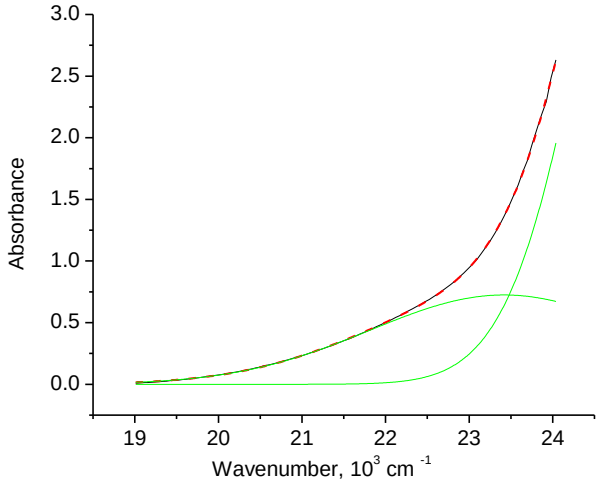

Fig. S2. Spectral deconvolution of the low-energy absorption (black) of the solution containing mixture of NPO and anthracene (see Fig. 1B) in dichloromethane

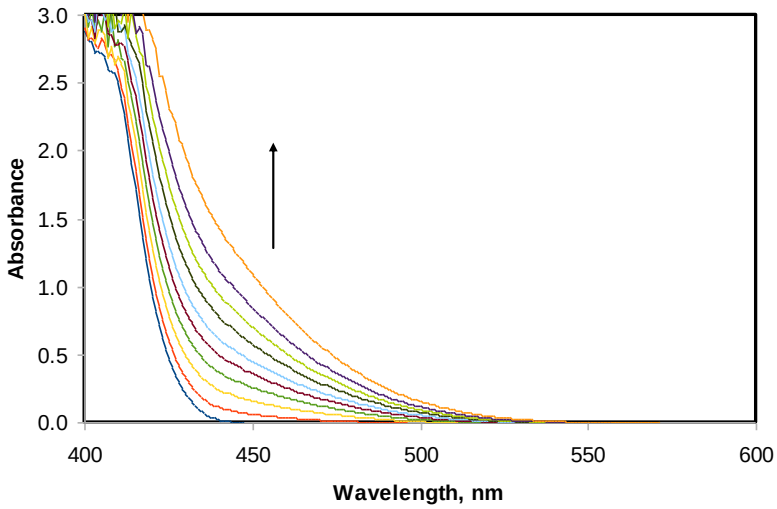

Fig. S3. Spectral changes occurring upon addition of pyrene to the solution of NPO in dichloromethane

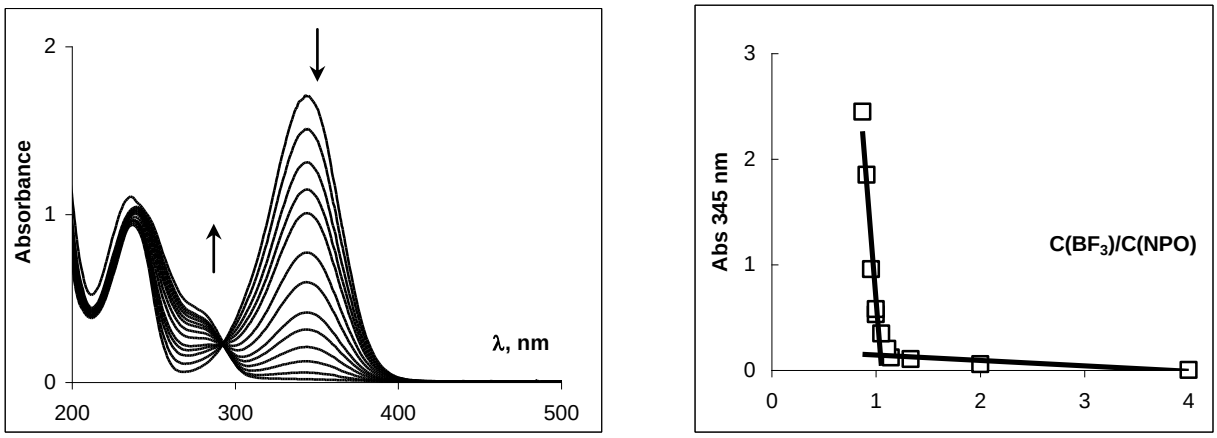

Fig. S4. Spectral changes occurring upon addition of BF_3 to the 0.1 mM solution of NPO in acetonitrile (left) and upon titration of NPO with BF_3 in dichloromethane (indicating the ratio BF_3/NPO = 1).

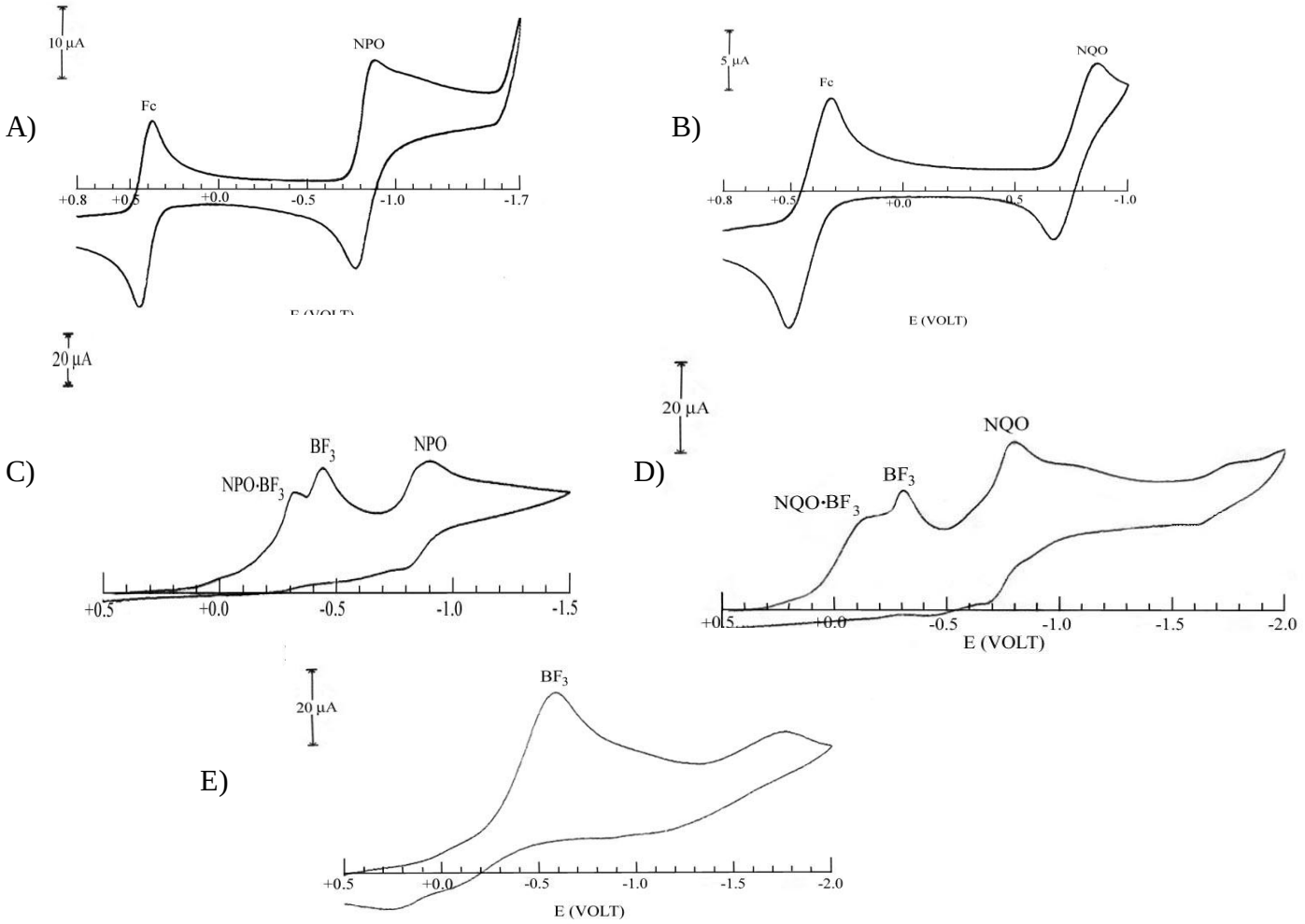

Fig. S5. Cyclic voltammogramms of the dichloromethane solutions of NPO (A) and NQO (B) mixture of NPO and BF_3 (C) mixture of NQO and BF_3 (D) and BF_3 (E). (Note that first waves in Figures A and B correspond to Fc^+/Fc internal standard).

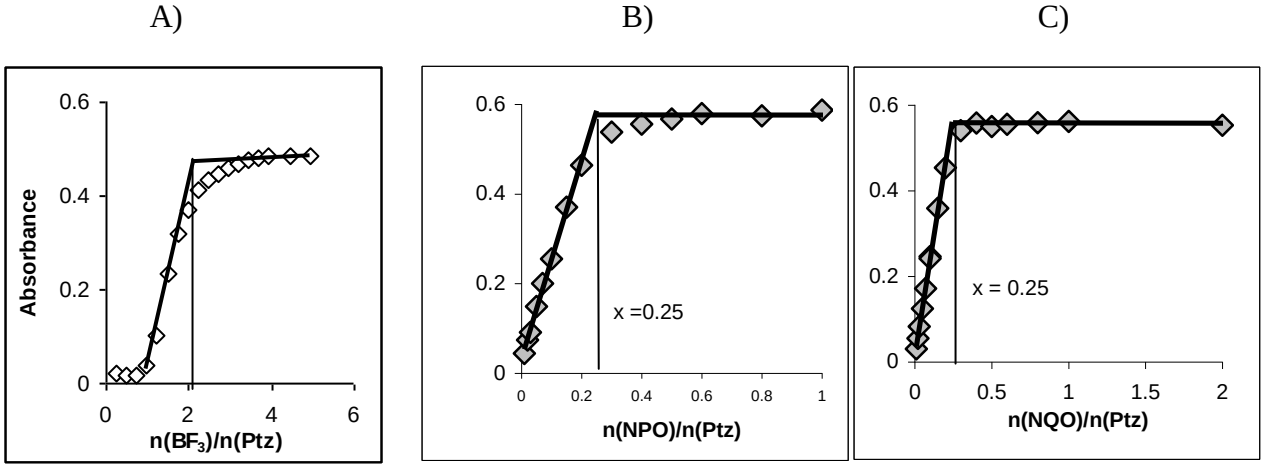

Fig. S6. Absorbance (λ = 745 nm) of the solutions with various PTZ:NXO:BF_3 ratios which indicate: (A) stoichiometric ratio BF_3/PTZ= 2 ($C_{PTZ} = C_{NPO}$ = 6.4 mM and various concentration of BF_3), (B) stoichiometric ratio PTZ/NPO = 4 (solutions with C_{PTZ} = 0.75 mM, C_{BF3} = 0.015 M and various concentrations of NPO); and (C) stoichiometric ratio PTZ/NQO = 4 (solutions with C_{PTZ} = 0.75 mM, C_{BF3} = 0.015 M and various concentrations of NQO). Note that absorption was measured in dichloromethane (l = 0.1cm) 24 h after component mixing, and λ = 745 nm corresponds to band maximum of phenothiazine cation radical.

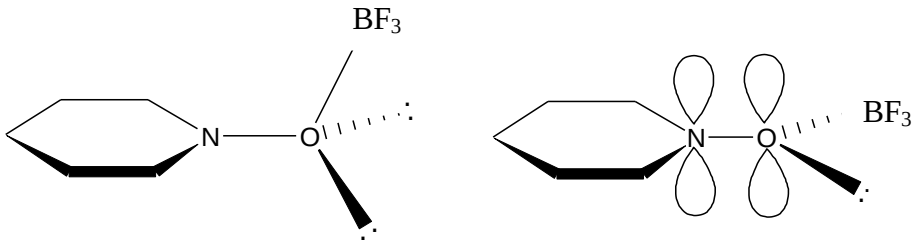

(A) (B)

Fig. S7. Illustration of BF_3-coordinated N-oxide molecules with sp^3 (A) and sp^2 (B) hybridization of oxygen atoms which shows that the C-N-O-B dihedral angle is close to zero in A, while steric and electronic factors favor staggered conformation and large dihedral angle in B. Note that the use of N-O-B angle as the indicator of the oxygen hybridization is hindered by its sensitivity to steric factors. Indeed, the data in in Table S6 demonstrate that analogous angles in the complexes of N-oxide of trimethylamine with various acceptors approach 109,5 deg (characteristic for sp^3-hybridization) only in the case of HCl, and in many cases these angles exceed 120 deg.

Table S6. Reported N–O–A angles for complexes of trimethylamine N-oxide with various acceptors

N	Acceptor	CSD refcode	angle, deg
1	-	TMEAMO	-
2	HCl	TMOHCL	109.88
		TMOHCL01	110.40
3	Pentachlorophenol	WOLZUS	104.26
4	Pentachlorophenol · H_2O	WOMBAB	107.79
5	$Al(CH_3)_3$	WAWKEK	127.21
6	$ZnCl_2$	TAPHAT	124.56
			122.06
7	$ZnBr_2$	TAPHEX	124.75
8	ZnI_2	FIQBIQ	124.99
9	CoI_2	TAPGUM	125.25

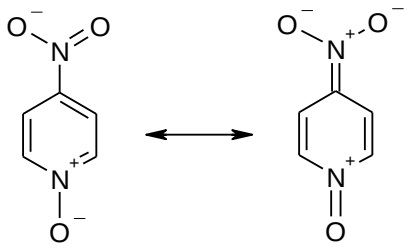

A B

Fig. S8. Benzenoid (A) and quinonoid (B) contributors to the 4-nitro-N-oxie structure.